BMC Genomics

RESEARCH

Open Access

Abnormal DNA methylation of *EBF1* regulates adipogenesis in chicken

Xiaohuan Chao[2,3,4], Lijin Guo[1,2,3], Meiling Hu[3], Mao Ye[1], Zhexia Fan[1], Kang Luan[1], Jiahao Chen[4], Chunlei Zhang[4], Manqing Liu[1,2,3], Bo Zhou[4], Xiquan Zhang[1,2,3], Zhenhui Li[1,2,3*] and Qingbin Luo[1,2,3*]

Abstract

Background DNA methylation influences gene expression and is involved in numerous biological processes, including fat production. It is involved in lipid generation in numerous animal species, including poultry. However, the effect of DNA methylation on adipogenesis in chickens remains unclear.

Results A total of 12 100-day-old chickens were divided into high and low-fat groups based on their abdominal fat ratios. Subsequently, genome-wide bisulfite sequencing (WGBS) was performed on their abdominal fat, and 1877 differentially methylated region (DMR) genes were identified, among which *SLC45A3*, *EBF1*, *PLA2G15*, and *ACAD9* were associated with lipid metabolism. Interestingly, *EBF1* showed a lower level of DNA methylation and higher mRNA expression in the low-fat group, as determined by comprehensive RNA-seq analysis. Cellular verification showed that *EBF1* expression was upregulated by 5-azacytidine (5-Aza) and downregulated by betaine. *EBF1* facilitated the differentiation of immortalized chicken preadipocyte 1 (ICP-1) through the PPAR-**γ** pathway, thereby affecting chicken adipogenesis.

Conclusion A combination of WGBS and RNA-seq analyses revealed 48 DMGs in the abdominal fat tissue of chickens. Notably, the DNA methylation status of *EBF1* was inversely related to its mRNA expression. Mechanistically, DNA methylation regulates *EBF1* expression, which in turn mediates the differentiation of ICP-1 through the PPARγ pathway. This study provides a theoretical framework for investigating the effects of DNA methylation on adipogenesis in chickens.

Keywords WGBS, Adipogenesis, DNA methylation, DMGs, *EBF1*

Background

The growing concern about obesity as a global health issue has been exacerbated by its increasing prevalence [1, 2]. According to statistics, in 2015, 107.7 million children and 603.7 million adults were obese [3]. The prevalence of obesity has doubled in over 70 countries since 1980, with a continuous upward trend observed in the majority of other countries [4]. Obesity has been identified as a warning signal for a range of diseases, including diabetes [5, 6], cardiovascular disease-related chronic diseases [7–9], osteoarthritis [10, 11], and even cancer [12, 13] The formation and deposition of fat involves a

*Correspondence:
Zhenhui Li
lizhenhui@scau.edu.cn
Qingbin Luo
qbluo@scau.edu.cn
[1]College of Animal Science, South China Agricultural University, Guangzhou, China
[2]State Key Laboratory of Livestock and Poultry Breeding, South China Agricultural University, Guangzhou, China
[3]Guangdong Provincial Key Lab of Agro-Animal Genomics and Molecular Breeding and Key Lab of Chicken Genetics, Breeding and Reproduction, Ministry of Agriculture, Guangzhou, China
[4]College of Animal Science and Technology, Nanjing Agricultural University, Nanjing, China

variety of factors, including alterations in gene expression and pathway network regulation related to lipogenesis and metabolism [14].

Adipose tissue plays a pivotal role in lipid deposition and metabolism, serving not only as an energy reserve but also as a vital endocrine and metabolic organ [15, 16]. Epigenetic modification is a significant factor in cell differentiation, development, gene expression regulation, and disease occurrence [17–19]. DNA methylation represents a form of epigenetic modification, and an increasing number of studies have demonstrated that DNA methylation plays a pivotal role in the process of adipose tissue formation and deposition in chickens [20–24]. For example, studies comparing the whole genome methylation of the backfat tissue of Landrace pigs (leaner) and Rongchang pigs (fatty) revealed, that the promoters of *PLIN1*, *BDKRB2*, *NSDHL*, *APOL1* and *APOL4* in lean backfat tissue were hypermethylated (93.75%) [25]. It has been demonstrated that DNA methylation in the *PLIN1* promoter region regulates *PLIN1* expression in chickens [26]. Zhang *et al.* demonstrated that the transcription of *KLF7* in chicken abdominal adipose tissue may be inhibited by promoter DNA methylation [27]. Cui *et al.* have demonstrated that *P1* methylation enhances *PPARγ1* expression, at least in part, by impeding the binding of *NRF1* to the *P1* promoter [28]. In poultry, approximately 85% of commercial broilers accumulate excess adipose tissue, particularly abdominal fat, which negatively impacts the efficiency of chicken production [29]. The public tends to prefer low-fat chickens because a high-fat chicken diet can encourage weight gain and pose a threat to public health. Therefore, research on obesity in chicken models serves two purposes, to gain new insights into the mechanism of fat deposition and to provide possible remedies to the public obesity problem. Regarding meat quality traits, some researchers have combined WGBS and RNA-seq to identify differences in chicken intramuscular fat [30], but no similar studies have been conducted to investigate the impact of DNA methylation of *EBF1* on chicken adipogenesis.

The transcription factor *EBF1* is a key regulator of B cell development and maturation [31]. Furthermore, studies have demonstrated that *EBF1* is a pivotal factor in the regulation of mature adipocyte metabolism and the development of brown fat [32, 33]. However, the precise role of DNA methylation of *EBF1* in the deposition of abdominal fat in chickens remains uncertain. This study aimed to explore the role of DNA methylation in abdominal fat deposition in chickens using WGBS. The present study demonstrates, for the first time that DNA methylation and *EBF1*expression are associated with fat deposition. The combined analysis of RNA-seq and WGBS revealed that *EBF1* had a higher degree of DNA methylation modification and lower mRNA expression in the high-fat group. Sequencing data demonstrated the potential role of DNA methylation of *EBF1* in abdominal fat deposition in chickens and provided a foundation for further studies on the genetic regulation mechanism of fat deposition.

Results

Output and quality control of WGBS data for abdominal fat tissue

To elucidate the epigenetic mechanism underlying abdominal fat deposition, abdominal fat tissues from six high-fat (HF) and low-fat (LF) groups were collected for WGBS. A total of 233.5G (average of 38.9G per sample) and 245.9G (average of 41.0G per sample) raw data were generated in the two groups of WGBS (Table 1). After quality control, the Q30 value was > 0.86. Unique mapped reads of the HF and LF groups accounted for 74% and 73.8% of the chicken genome, respectively. The average sequencing depth was approximately 30× (Fig. 1A). The effective coverage of CpG sites was approximately 80%

Table 1 The summary of data generated by genome-wide bisulfite sequencing

Samples	Raw reads	Raw bases (G)	Clean reads	Clean bases (G)	Clean Q30 Bases Rate(%)	Mapped Reads	Mapped Ratio (%)	Unique Mapped Reads	Unique Mapped Ratio(%)
HF1	257,266,250	38.6	247,780,782	37.2	88.03	188,709,464	76.16	186,494,542	75.3
HF2	271,670,374	40.8	260,846,236	39.1	89.4	194,095,176	74.41	192,093,452	73.6
HF3	243,000,918	36.5	233,080,882	35	87.84	173,417,556	74.4	171,375,900	73.5
HF4	281,066,904	42.2	271,644,800	40.7	88.3	207,567,834	76.41	205,063,956	75.5
HF5	263,637,888	39.5	251,558,724	37.7	89.47	186,918,234	74.3	185,035,114	73.6
HF6	239,692,892	36	232,140,290	34.8	90.41	170,403,884	73.41	168,142,214	72.4
LF1	219,016,470	32.9	209,983,650	31.5	90.21	161,957,256	77.13	159,957,366	76.2
LF2	270,959,478	40.6	257,890,644	38.7	86.61	186,544,812	72.33	184,244,888	71.4
LF3	302,452,046	45.4	289,669,886	43.5	87.61	218,754,046	75.52	216,186,458	74.6
LF4	253,064,090	38	243,479,716	36.5	89.39	187,073,572	76.83	184,754,824	75.9
LF5	287,761,978	43.2	274,251,108	41.1	87.18	201,119,304	73.33	198,522,844	72.4
LF6	306,383,992	46	292,071,680	43.8	86.62	213,966,026	73.26	211,387,184	72.4

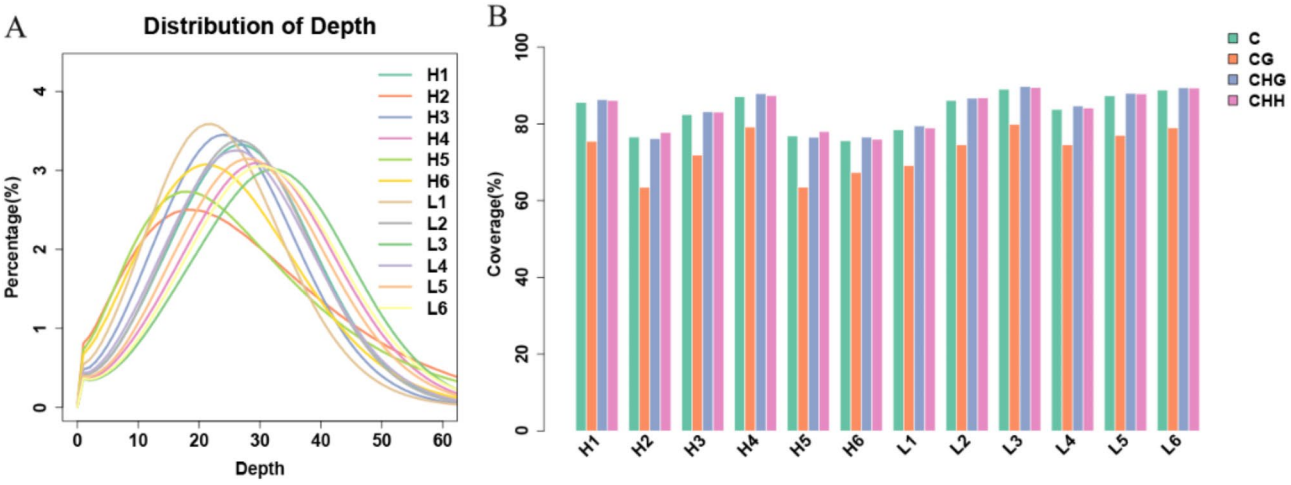

Fig. 1 Quality analysis of DNA methylation data in chicken between the high-fat and low-fat groups. (**A**) The average sequencing depth. (**B**) The effective coverage of CpG sites

(Fig. 1B and Supplementary File 1: Tables S1, and S2). These findings suggested the reliability of the sequencing outcomes.

Global DNA Methylation Patterns in high and low-fat chickens

In LF chicken abdominal fat tissue, the number of cytosines in the CHG and CHH hypermethylated states (50-100%) was greater than that in HF chicken, whereas the opposite was true in the hypomethylated state (10-50%). The number of CG-type cytosine in HF chicken abdominal fat tissue containing "bumps" in the region close to 100% methylation, was significantly higher than that in the LF (Fig. 2A). The total DNA methylation levels of cytosine (C) in the HF and LF chickens were 3.35% and 3.40%, respectively (Table 2). In HF broilers, 58.40% CG, 0.67% CHG, and 0.68% CHH were methylated, whereas in LF broilers, 58.95% CG, 0.65% CHG, and 0.65% CHH were methylated. A comparison of the overall methylcytosine content of HF and LF indicates that LF exhibits a higher level of methylation than HF. However, the proportion of CG, CHG, and CHH in HF and LF is found to be similar. (Figure 2B and C). The results of the motif analysis indicate that there was no preference for bases near methylated cytosines between HF and LF. However, the methylated cytosines exhibited a preference for being located in CHG and CHH (H = A > T). (Fig. 2D).

Functional characterization of differentially methylated genes (DMGs)

A total of 1877 differentially methylated regions (DMRs) were identified (Supplementary File 1: Table S3). The circos map displays the P-values of the DMRs, the number of DMRs, and the average methylation levels of differences in the chicken chromosomes (1–33 and Z) (Fig. 3A). A statistical analysis of the location of DMRs in adipose tissue revealed that the majority of DMRs are situated in intron and distal intergenic regions, followed by exon. A small number of DMRs were also identified in other regions (Fig. 3B). Of these DMRs, 56.05% were hypomethylated and 43.95% were hypermethylated in HF chicken abdominal fat tissue. The average length of DMRs was approximately 200 bp (Fig. 3D). In order to investigate the potential biological role of DMGs, a total of 1455 DMGs were analyzed using the Gene Ontology (GO) and Kyoto Encyclopedia of Genes and Genomes (KEGG) pathways. The findings of this study revealed that the DMGs were primarily enriched in integral components of the membrane, the nucleus, ATP binding, metabolic pathways, calcium signaling pathways, mitogen-activated protein kinase (MAPK) signaling pathways, the regulation of actin cytoskeleton, and the Wnt signaling pathway (Fig. 3C and E). In addition, several fat-related pathways were enriched (Supplementary File 1: Table S4). Among these, *SLC45A3*, *EBF1*, *PLA2G15*, and *ACAD9* were found to be associated with lipid metabolism.

Comprehensive analysis of RNA-Seq and WGBS

To explore whether the candidate DMGs were related to abdominal fat deposition, we comprehensively analyzed the WGBS and RNA-Seq data obtained from the same sample in our previous study [34]. RNA-Seq results showed that many lipid-related genes, such as *LPIN1*, *MOGAT2*, *DGAT2*, *ABHD5*, *ACBD5*, and *FABP1* were differentially expressed. Our comprehensive analysis revealed 12 (hypermethylated and significantly down-regulated) and 22 (hypomethylated and significantly up-regulated) DMR genes in the abdominal fat tissue of HF and LF groups (Fig. 4A). A cluster analysis of differentially methylated differential genes revealed that 26 genes were up-regulated and 22 genes were down-regulated in HF groups (Fig. 4B). GO enrichment analysis of

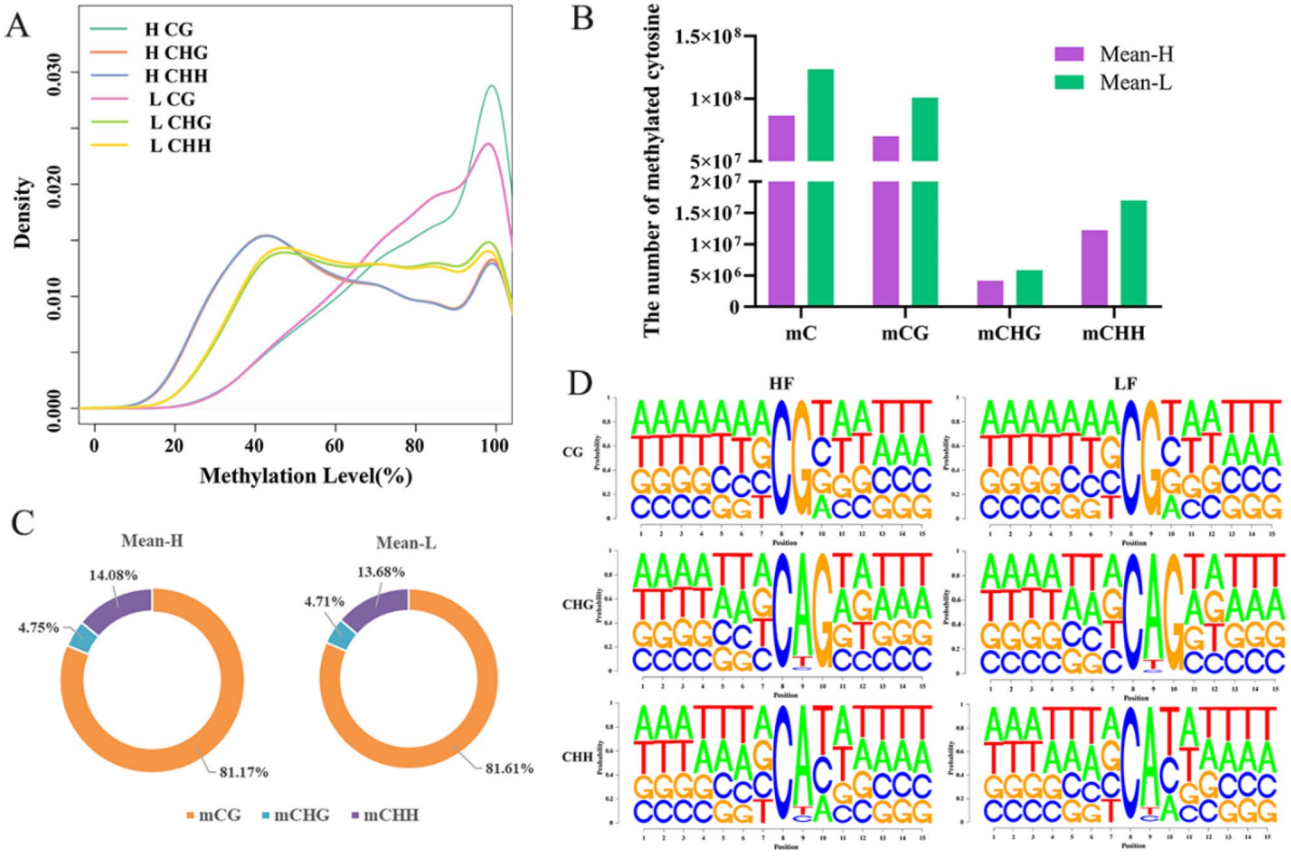

Fig. 2 Preference for methylated cytosine between the High-fat and Low-fat groups. (**A**)The number of cytosine analyses of CG, CHG, and CHH. (**B**, **C**) Analysis of the proportion of CG, CHG, and CHH. (**D**) Markedly different motif types in the High-fat group and the Low-fat groups

Table 2 Total methylation level statistics of abdominal lipid genome

Sample	C(%)	CG(%)	CHG(%)	CHH(%)
HF1	3.41	58.20	0.70	0.70
HF2	3.25	59.10	0.70	0.70
HF3	3.34	58.00	0.60	0.70
HF4	3.45	57.90	0.70	0.70
HF5	3.30	60.30	0.70	0.70
HF6	3.32	56.90	0.60	0.60
LF1	3.37	58.50	0.60	0.60
LF2	3.30	58.00	0.60	0.60
LF3	3.35	57.70	0.70	0.70
LF4	3.50	59.60	0.70	0.70
LF5	3.40	59.40	0.60	0.60
LF6	3.49	60.50	0.70	0.70
Mean-HF	3.35	58.40	0.67	0.68
Mean-LF	3.40	58.95	0.65	0.65
P	0.228	0.414	0.599	0.26

differential genes with differential DNA methylation was performed. A review of the top ten enrichment items reveals that the primary enrichment is observed in metal ion binding, positive regulation of transcription, and positive regulation of transcription (Fig. 4C). Protein-protein interaction (PPI) network analysis revealed a strong correlation between these genes (Fig. 4D). Studies have shown that *EBF1* is associated with fat development [32, 33]. In the HF group, *EBF1* methylation lever exhibited a significant decrease in methylation, while mRNA expression exhibited a significant increase.

Methylation inhibits *EBF1* expression and *EBF1* inhibits preadipocyte the differentiation

Sequencing analysis revealed that *EBF1* methylation was negatively correlated with its expression level. Following treatment of the cells with 5-Aza-dc, demethylation of the modification site was observed through Bisulfite treatment and Sanger sequencing (Fig. 5A). After the cells were treated with 5-Aza-dc and betaine, the qPCR results revealed that *EBF1* expression was negatively correlated with the degree of methylation modification, and *EBF1* expression decreased as the degree of methylation modification increased (Fig. 5B and C). Furthermore, the qPCR results revealed that *EBF1* was differentially expressed in the HF and LF groups (Fig. 5D). *EBF1* was enriched in PPARA activated genes. To further investigate the role of *EBF1* in fat deposition, sodium oleate was used to induce ICP-1 differentiation, and *EBF1*

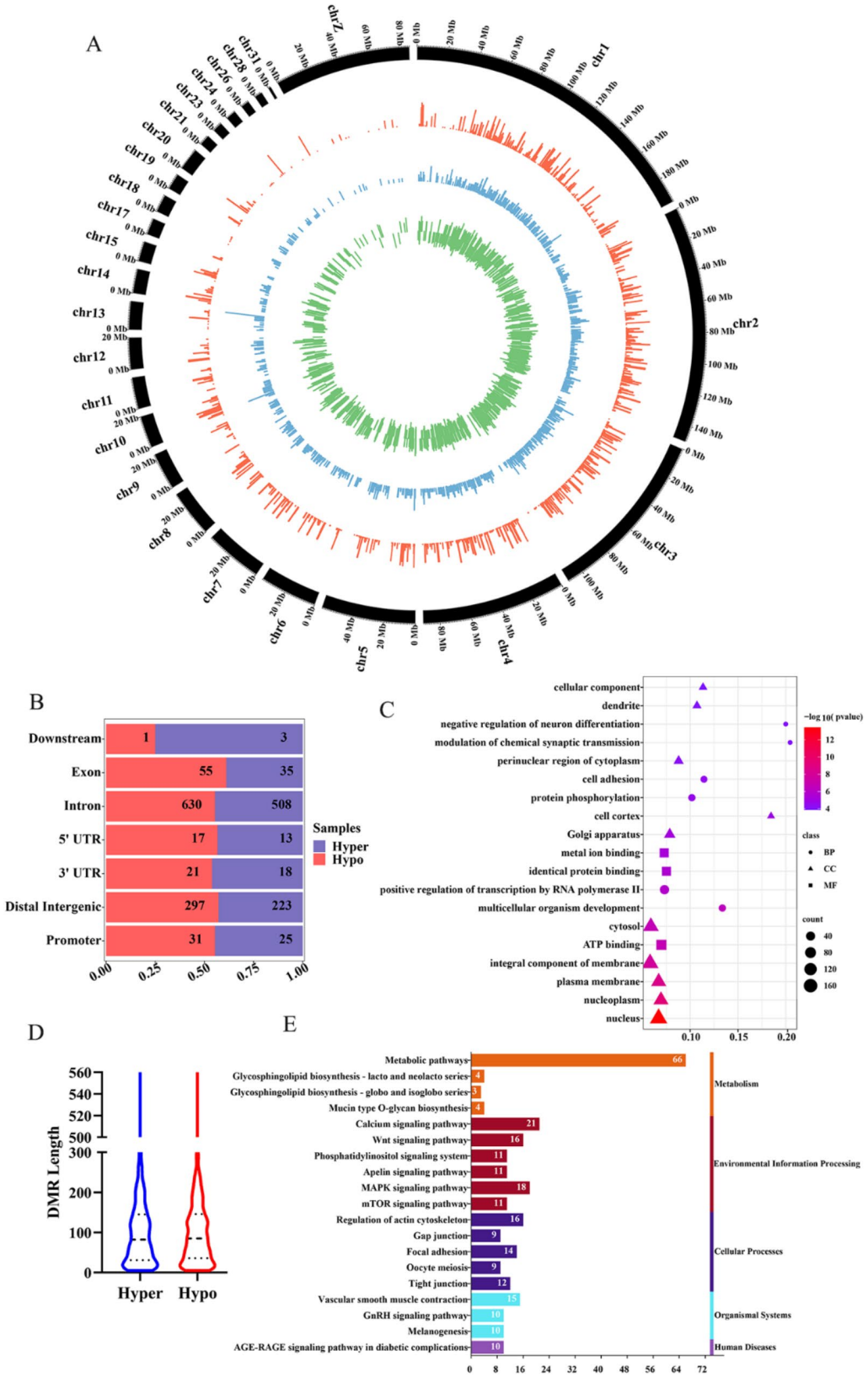

Fig. 3 Functional analysis of differentially methylated genes. (**A**) The distribution of DMRs on chromosomes (**B**) Location analysis of differentially methylation regions. (**D**) The average length of DMGs. (**C**, **E**) The GO enrichment analysis and KEGG pathways of DMGs

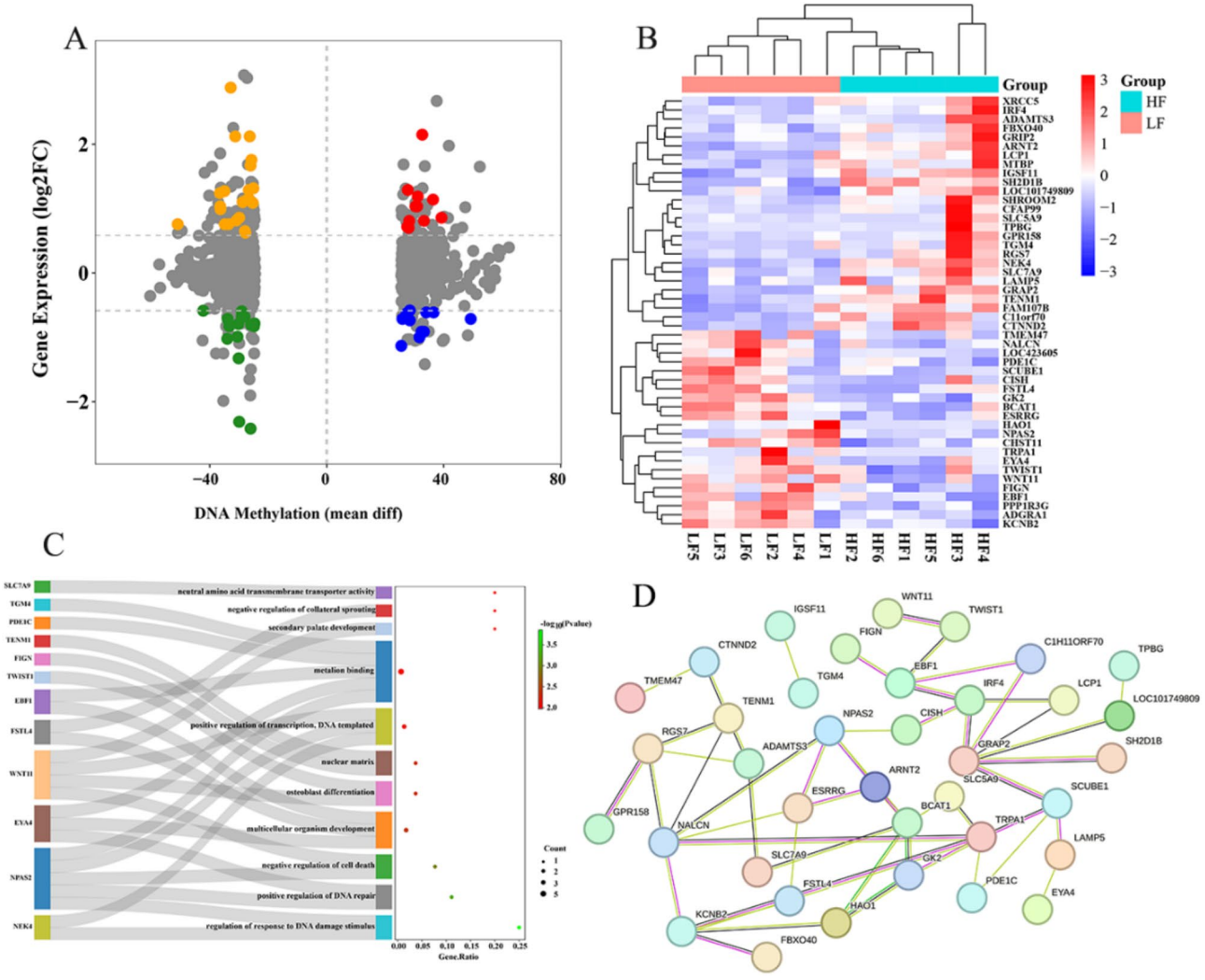

Fig. 4 Combined analysis of RNA-seq and WGBS. (**A**) Four quadrants between differential expression genes and DMGs. (**B**) A cluster analysis of differential genes with differential DNA methylation was conducted. (**C**) The GO was performed for differential genes with differential DNA methylation. (**D**) PPI analysis was performed on differential genes with differential DNA methylation

expression of mRNA and protein decreased following differentiation (Fig. 5E and F). Oil red staining revealed that *EBF1* inhibited preadipocyte differentiation (Fig. 5G-I). In addition, qPCR results showed that the expression of differentiation-related genes *PPARγ*, *C/EBPα*, *C/EBPβ*, *ADIPOR1*, and *LPL* decreased after overexpression of *EBF1* (Fig. 5J). At the protein level, *EBF1* inhibited PPARγ expression, suggesting that *EBF1* inhibited adipose differentiation through the PPARγ axis (Fig. 5K).

Discussion

Abdominal fat deposits have been linked to several disorders, and research has indicated that DNA methylation plays a significant role in the metabolism of adipose tissue and lipids in a range of animals, including chickens [25, 30]. In this study, WGBS sequencing revealed differential DNA methylation modifications, of *EBF1*. A combined analysis using previously studied RNA-seq data revealed that *EBF1* had a higher level of DNA methylation in the low-fat group but lower mRNA expression. Based on sequencing data, we validated the cell function of *EBF1* and found that DNA methylation affects its expression. 5-Aza-dc has been demonstrated to inhibit DNA methyltransferase and promotes *EBF1* expression, whereas betaine inhibits *EBF1* expression. Moreover, our findings indicate that *EBF1* plays a regulatory role in the differentiation of precursor adipocytes through the PPAR-β signaling pathway.

To explore the relationship between DNA methylation and abdominal fat deposition in chickens, we compared whole-gene methylation in abdominal adipose tissues from the HF and LF groups. Our finding indicate that HF chickens exhibited lower overall methylation levels than LF chickens. This result contradicts Gong's findings [35]. It has been

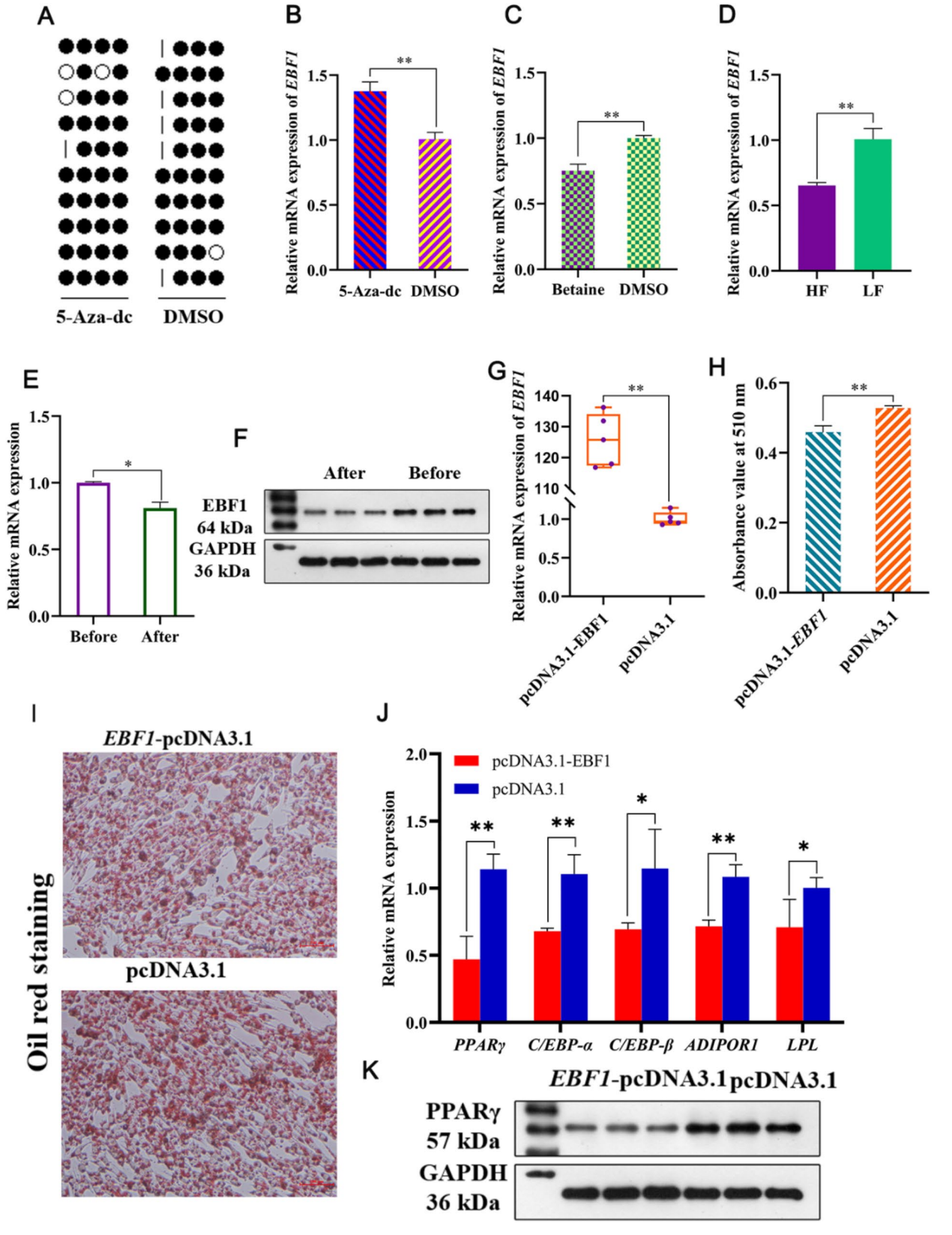

Fig. 5 (See legend on next page.)

(See figure on previous page.)

Fig. 5 The DNA methylation of *EBF1* affects adipogenesis differentiation. (**A**) DNA methylation levels of cells treated with 5-Aza-dc and DMSO. (**B**, **C**) Cells were treated with 5-Aza-dc and betaine to detect the relative expression of EBF1. (D) Relative expression of *EBF1* in High-fat chicken and Low-fat chicken. (**E**, **F**) The expression of mRNA and protein in EBF1 before and after the differentiation of preadipocytes was investigated. (**G**) Detection of transfection efficiency of *EBF1*. (**H**, **I**) Oil red staining showed the influence of *EBF1* on grease drops. (**J**) Relative mRNA expression of *PPARγ*, *C/ EBPα*, *C/ EBPβ*, *ADIPOR1*, and *LPL* in ICP-1 cells. (**K**) Western blot for PPARγ protein in ICP-1 cells after EBF1 transfection, full-length blots are presented in Supplementary file 2 A. Data presented as mean ± SEM, **P* < 0.05; ***P* < 0.01; ns: no significance

demonstrated that the levels of DNA methylation of specific genes fluctuate with age [36, 37]. In the study conducted by Gong *et al*., chickens at seven weeks of age were utilized, whereas in the present experiment, chickens at 100 days of age were employed. It can therefore be hypothesized that the alterations in DNA methylation levels of specific genes resulting from the age discrepancy between the chickens may be the underlying cause of the observed overall difference. The DNA methylation pattern observed in this study was predominantly GC, which is in accordance with the findings of Luo *et al.* [38]. Additionally, the majority of the differential DMRs were identified within introns, a result that aligns with the conclusions of Lu *et al.* [39]. The study by Wang et al. demonstrated that DMRs are predominantly located at the 5' end in liver lipid metabolism. In contrast, this study revealed that they are primarily situated within introns [40]. Given that DNA methylation is susceptible to environmental influences, Wang *et al.* employed a high-fat diet and a low-fat diet to construct their model. In contrast, this experiment employed a normal feeding regimen, which may be a contributing factor to the observed discrepancy in the predominant DMR locations.

EBF1 plays a pivotal role in regulating lipid metabolism [41–43]. Although previous studies have demonstrated that abnormal DNA methylation of *EBF1* is associated with various diseases [43–45]. To date, no study has focused on its role in fat deposition. This study demonstrated for the first time that DNA methylation of *EBF1* is associated with fat deposition. Abnormal DNA methylation of *EBF1* was identified in the WGBS of abdominal adipose tissue in both high and low-fat groups, with a lower level of DNA methylation in the low-fat group. Treatment of ICP cells with 5-Aza-dc was observed to promote *EBF1* expression, whereas treatment with betaine was seen to inhibit *EBF1* expression. The experiments conducted by Napat Armartmuntree and colleagues demonstrated a negative correlation between DNA methylation of *EBF1* and mRNA expression, which was consistent with the sequencing results of this experiment [46]. Studies have shown that *EBF1* expression is linked to lipid metabolism and is enriched in the PPARγ pathway [47], Therefore, we investigated their biological roles. Using qPCR, oil red staining, and protein analysis, we found that *EBF1* inhibited adipocyte differentiation via the PPARγ pathway. Yasmina *et al.* showed that miR-365-5p and miR-574-5p were highly expressed in obese adults and that miR-365-5p and miR-574-5p could target *EBF1* and reduce its expression, which was consistent with our reduced expression of *EBF1* in the high-fat chicken group [48]. Masaaki *et al*. showed that miR-33b affects the differentiation and development of porcine precursor adipocytes by decreasing the expression of *EBF1*, *C/EBPα*, and *PPARγ* lipid genes, which is contrary to our findings that EBF1 inhibits adipocyte differentiation via through the PPARγ pathway [49]. This could be attributed to species differences or to DNA methylation. Further investigation is required to determine the specific reasons for these differences.

Conclusion

In summary, our findings indicate that *EBF1* expression and the level of DNA methylation differ in the low-fat group. In addition, cytological experiments revealed that DNA methylation of *EBF1* affects *EBF1* expression. *EBF1* also regulates ICP-1 differentiation via the PPARγ pathway. The findings of this study provide a theoretical framework for investigating the effects of DNA methylation on adipogenesis.

Materials and methods

Animal experiment and ethics statement

The animals used in this study were supported by Wens. 158 Sanhuang broilers were put in a cage after birth and were fed ad libitum. When they reach the age of 100 days, they were euthanized by cervical dislocation. Weight and abdominal fat weight were measured. The abdominal fat tissues were collected and stored in a refrigerator at -80 °C. According to the abdominal fat rate (abdominal fat rate = abdominal fat weight/live weight*100%), Twelve individuals were selected and divided into high-fat group (HF) and low-fat group (LF), with 6 in each group. The measurement data of 12 individuals are shown in Table 3. The animal experiments conducted in this study were approved (license ID: SCAU#2017015; September 13, 2017) by the Animal Care Committee of South China Agricultural University.

Whole-genome bisulfite sequence (WGBS)

Twelve 100-day-old ad libitum Sanhuang broilers were euthanized, and their abdominal fat tissues were collected. DNA extracted from the 12 abdominal fat tissues, were sent to Annoroad Gene Technology (Beijing) Co., Ltd. for WGBS.

DNA extraction and total RNA extraction

The DNA was extracted using DNA extraction kit (TAKARA, Japan) according to the manufacturer's

Table 3 Abdominal fat rate of 12 experimental chickens

Individual ID	Weight(g)	Abdominal fat weight(g)	Abdominal fat rate(%)
HF1	1602.5	128.8	8.04
HF2	1747.2	146.5	8.38
HF3	1415.8	119.9	8.47
HF4	1735.5	151.6	8.74
HF5	1618.9	155.5	9.61
HF6	1839.7	179.4	9.75
Mean ± SD	1659.93 ± 60.61	146.95 ± 8.58**	8.83 ± 0.28**
LF1	1705.9	66.4	3.89
LF2	1550	56.8	3.66
LF3	1360	50.3	3.7
LF4	1564.8	58.2	3.72
LF5	1419.9	55.6	3.92
LF6	1235.2	34.7	2.81
Mean ± SD	1472.63 ± 68.49	53.67 ± 4.35	3.62 ± 0.17

instructions. MagZol Reagent (Magen, Guangdong, China) was used for extracting total RNA from abdominal fat tissues and cells according to the manufacturer's instructions.

Bisulfite treatment and Sanger sequencing

Primers are designed by Methyl Primer Express v1.0. The DNA was extracted and amplified. Following the recovery of the PCR amplification products by cutting the glue, they were connected to the T vector with the use of a TA cloning kit. The connected products were then transformed into coated plates, after which the monoclonal plaque was sent to the sequencing department for sequencing. A total of 10 monoclones were selected from each plate for sequencing.

Reverse transcription and Real-time quantitative PCR (RT-qPCR)

To validate the gene expression changes, total RNA was reverse transcribed using PrimescriptTM RT Reagent Kit with gDNA Eraser (Takara, Japan), and qRT-PCR was performed with ChamQ Universal SYBR qPCR Master Mix (Vazyme, Nanjing, China). qRT-PCR was performed using ABI QuantStudio 5 instrument (Thermo Fisher, NY, USA). Relative expression was calculated using GAPDH as a reference gene and comparative cycle threshold method ($2^{-\Delta\Delta Ct}$). The primers used in qPCR were designed by Premier Primer 5.0 software and the primer sequences are listed in Supplementary file 1: Table S5.

Data analysis of differential methylation genes

The software and parameters used in the align of the WGBS data refer to the paper published by Krueger and Andrews [50]. GCF_016700215.2 is used as the reference genome (downloaded from https://download.cncb.ac.cn/assembly/ncbi/Animals/GCF/016/700/Gallus_gallus_chicken_bGalGal1.pat.whiteleghornlayer.GRCg7w_WZ_GCF_016700215.2/GCF_016700215.2_bGalGal1.pat.whiteleghornlayer.GRCg7w_genomic.fna.gz, and the matching annotation file is downloaded from https://download.cncb.ac.cn/assembly/ncbi/Animals/GCF/016/700/Gallus_gallus_chicken_bGalGal1.pat.whiteleghornlayer.GRCg7w_WZ_GCF_016700215.2/GCF_016700215.2_bGalGal1.pat.whiteleghornlayer.GRCg7w_genomic.gff.gz). Methylation level difference more than 40% and q value ≤ 0.05 were considered as the cut off differentially methylated C sites (DMC). DMR analysis was performed by R package methylKit.V.0.9.2 [51] and eDMR.V.0.5.1 [52], and the standard is that the coverage depth of a single site is at least 10 on the same genomic location in multiple samples, contains at least 4 CpGs and 1 DMC, and one area with an average differential methylation level greater than 25%. We define the DMGs as the genes that overlap with the location of DMR.

GO/KEGG enrichment analysis and PPI network analysis

We performed Gene Ontology (GO) analysis and KEGG enrichment analysis for DMGs. PPI analysis is carried out in STRING (https://string-db.org/).

Cell culture and cell transfection

ICP-1 was cultured in a mixture of DMEM and DMEM/F12 (Gibco, CA, United States) mixed with 15% fetal bovine serum (Gibco, CA, United States) and 1% streptomycin/penicillin. And then put it in an incubator 37℃ and 5% CO_2 (Invitrogen, CA, United States, United States). The plasmids transfection was performed according to Lipofectamine 3000 (Invitrogen, CA, United States) instructions. Transfection doses for 12-well plate was 1 μg/ well.

Plasmids construction

The complete CDS sequence of *EBF1* (NM_001397656.1) was subcloned into the Nhe I and Kpn I sites of the pcDNA3.1 vector (Promega, WI, United States) by TSINGKE (Beijing, China), and then named pcDNA3.1-*EBF1*.

Oil red O staining

A medium with 15% fetal bovine serum and 0.2% oleic acid (Sigma, CA, United States) was used to induce preadipocyte differentiation after 6 h of transfection. 300 μL of 4% paraformaldehyde was used to fix the cells at room temperature for 30 min after induction for 48 h. Then, the Oil red staining test was carried out according to the Oil Red O Staining Solution (SolarBio, Beijing, China) instructions.

Western blotting

After 48 h of transfection, proteins were extracted from cells. Extract proteins from cells. Protein samples were isolated on 10% SDS-PAGE gel (EpiZyme, Shanghai, China) and transferred to a polyvinylidene fluoride (PVDF) membrane (Bio-Rad, CA, United States). The membrane was placed in a bag with anti-PPARγ (1: 1,000; bs-0530R, BIOSS), anti-EBF1 (1: 1,000; bs-12116R, BIOSS) and anti-GAPDH antibodies (1: 2,000; bsm-33033 M, BIOSS) at 4℃ for 12 h. The film can be exposed by inserting it into an X-ray clamp. Finally, ImageJ software was used to measure the gray value (image density) of the strip.

Other data analysis

The data represents mean ± SEM. The sample size of each experiment is at least three. Student's t-test and ANOVA analysis were performed to determine the statistical significance of differences observed between groups. $^{*}P < 0.05$; $^{**}P < 0.01$; ns: no significance.

Abbreviations

WGBS	Genome-wide bisulfite sequencing
DMR	Differentially methylated region
5-Aza	5-azacytidine
ICP-1	Immortalized chicken preadipocyte 1
EBF1	EBF Transcription Factor 1
HF	High-fat
LF	Low-fat
GO	Gene Ontology
KEGG	Kyoto Encyclopedia of Genes and Genomes
DMGs	Differentially methylated genes
SLC45A3	Solute Carrier Family 45 Member 3
PLA2G15	Phospholipase A2 Group XV
ACAD9	Acyl-CoA Dehydrogenase Family Member 9
LPIN1	Phosphatidate Phosphatase LPIN1
MOGAT2	Monoacylglycerol O-Acyltransferase 2
DGAT2	Diacylglycerol O-Acyltransferase 2
ABHD5	Abhydrolase Domain Containing 5, Lysophosphatidic Acid Acyltransferase
ACBD5	Acyl-CoA Binding Domain Containing 5
FABP1	Fatty Acid Binding Protein 1
C/EBPα	CCAAT Enhancer Binding Protein Alpha
PPARγ	Peroxisome Proliferator-Activated Receptor Gamma

Supplementary Information

The online version contains supplementary material available at https://doi.org/10.1186/s12864-025-11464-6.

Supplementary Material 1: Table S1: Genome sequencing coverage statistics table. Table S2: Effective genomic C coverage of abdominal fat. Table S3: The information pertaining to DMRs. Table S4: KEGG analysis related to fat. Table S5: Primers sequence information.

Supplementary Material 2: A: Original Figure of Figure 5F, B: Original Figure of Figure 5K.

Acknowledgements

We would like to thank ICP-1 was provided by Li Hui laboratory of Northeast Agricultural University (Heilongjiang, China).

Author contributions

XH C, LJ G and ML H was involved in research design, data analysis and manuscript writing. K L, ZX F and M Y participated in the experiment and data analysis; ZH L and B Z reviewed the revised manuscript; JH C, CL Z, MQ L, and XQ Z were responsible for samples collection; QB L designed the entire study and supervised its progress.

Funding

This work was supported by the Key-Area Research and Development Program of Guangdong Province, No.2022B0202100002, Science and Technology Program of Guangzhou City No. 2024B03J1353, and Science and Technology Program of Chaozhou City No.202101ZD07.

Data availability

Sequencing data submitted in the NCBI database of SRA. Accession link: http://www.ncbi.nlm.nih.gov/bioproject/942033.

Declarations

Ethics approval and consent to participate

All methods were carried out in accordance with relevant guidelines and regulations. This study was carried out in compliance with the ARRIVE guidelines 2.0 (https://arriveguidelines.org/). All animals are euthanized in accordance with animal welfare. The animal experiment program was approved by the Animal Care Committee of South China Agricultura (SCAU#2017015; September 13, 2017).

Consent for publication

Not applicable.

Competing interests

The authors declare no competing interests.

Received: 10 May 2024 / Accepted: 10 March 2025
Published online: 20 March 2025

References

1. Chandler M, Cunningham S, Lund EM, Khanna C, Naramore R, Patel A, Day MJ. Obesity and associated comorbidities in people and companion animals: A one health perspective. J Comp Pathol. 2017;156(4):296–309.
2. Bristow C, Meurer C, Simmonds J, Snell T. Anti-obesity public health messages and risk factors for disordered eating: a systematic review. Health Promot Int. 2020;35(6):1551–69.
3. Roberto CA, Swinburn B, Hawkes C, Huang TT, Costa SA, Ashe M, Zwicker L, Cawley JH, Brownell KD. Patchy progress on obesity prevention: emerging examples, entrenched barriers, and new thinking. Lancet. 2015;385(9985):2400–9.
4. Collaborators GBDO, Afshin A, Forouzanfar MH, Reitsma MB, Sur P, Estep K, Lee A, Marczak L, Mokdad AH, Moradi-Lakeh M, et al. Health effects of overweight and obesity in 195 countries over 25 years. N Engl J Med. 2017;377(1):13–27.
5. Zerga AA, Bezabih AM, Adhanu AK, Tadesse SE. Obesity indices for identifying metabolic syndrome among type two diabetes patients attending their Follow-Up in Dessie referral hospital, North East Ethiopia. Diabetes Metab Syndr Obes. 2020;13:1297–304.
6. Qi W, Clark JM, Timme-Laragy AR, Park Y. Per- and polyfluoroalkyl substances and obesity, type 2 diabetes and Non-alcoholic fatty liver disease: A review of epidemiologic findings. Toxicol Environ Chem. 2020;102(1–4):1–36.
7. Singh GM, Danaei G, Farzadfar F, Stevens GA, Woodward M, Wormser D, Kaptoge S, Whitlock G, Qiao Q, Lewington S, et al. The age-specific quantitative effects of metabolic risk factors on cardiovascular diseases and diabetes: a pooled analysis. PLoS ONE. 2013;8(7):e65174.
8. Emerging Risk Factors C, Wormser D, Kaptoge S, Di Angelantonio E, Wood AM, Pennells L, Thompson A, Sarwar N, Kizer JR, Lawlor DA, et al. Separate and combined associations of body-mass index and abdominal adiposity with cardiovascular disease: collaborative analysis of 58 prospective studies. Lancet. 2011;377(9771):1085–95.
9. Pleis JR, Ward BW, Lucas JW. Summary health statistics for U.S. Adults: National health interview survey. Vital Health Stat. 2009;10 2010(249):1–207.
10. Jiang L, Tian W, Wang Y, Rong J, Bao C, Liu Y, Zhao Y, Wang C. Body mass index and susceptibility to knee osteoarthritis: a systematic review and meta-analysis. Joint Bone Spine. 2012;79(3):291–7.

11. Jiang L, Rong J, Wang Y, Hu F, Bao C, Li X, Zhao Y. The relationship between body mass index and hip osteoarthritis: a systematic review and meta-analysis. Joint Bone Spine. 2011;78(2):150–5.
12. Lauby-Secretan B, Scoccianti C, Loomis D, Grosse Y, Bianchini F, Straif K. International agency for research on cancer handbook working G: body fatness and cancer–Viewpoint of the IARC working group. N Engl J Med. 2016;375(8):794–8.
13. Avgerinos KI, Spyrou N, Mantzoros CS, Dalamaga M. Obesity and cancer risk: emerging biological mechanisms and perspectives. Metabolism. 2019;92:121–35.
14. Bugianesi E. Fatty liver disease: putting the spotlight on a silent menace for young adults. Lancet Gastroenterol Hepatol. 2020;5(3):236–8.
15. Sahu B, Bal NC. Adipokines from white adipose tissue in regulation of whole body energy homeostasis. Biochimie. 2023;204:92–107.
16. Giralt M, Cereijo R, Villarroya F. Adipokines and the endocrine role of adipose tissues. Handb Exp Pharmacol. 2016;233:265–82.
17. Chao X, Guo L, Ye C, Liu A, Wang X, Ye M, Fan Z, Luan K, Chen J, Zhang C, et al. ALKBH5 regulates chicken adipogenesis by mediating LCAT mRNA stability depending on m(6)A modification. BMC Genomics. 2024;25(1):634.
18. Gong X, Yu Q, Duan K, Tong Y, Zhang X, Mei Q, Lu L, Yu X, Li S. Histone acetyltransferase Gcn5 regulates gene expression by promoting the transcription of histone methyltransferase SET1. Biochim Biophys Acta Gene Regul Mech. 2020;1863(9):194603.
19. Chen X, Gong W, Shao X, Shi T, Zhang L, Dong J, Shi Y, Shen S, Qin J, Jiang Q, et al. METTL3-mediated m(6)A modification of ATG7 regulates autophagy-GATA4 axis to promote cellular senescence and osteoarthritis progression. Ann Rheum Dis. 2022;81(1):87–99.
20. Campion J, Milagro F, Martinez JA. Epigenetics and obesity. Prog Mol Biol Transl Sci. 2010;94:291–347.
21. Wan QL, Meng X, Wang C, Dai W, Luo Z, Yin Z, Ju Z, Fu X, Yang J, Ye Q, et al. Histone H3K4me3 modification is a transgenerational epigenetic signal for lipid metabolism in caenorhabditis elegans. Nat Commun. 2022;13(1):768.
22. Sun YN, Qiao YGSP, Wang SZ, Duan K, Wang YX, Li H, Wang N. Epigenetic DNA methylation in the promoters of Peroxisome Proliferator-Activated Receptor γ in chicken lines divergently selected for fatness. 2013.
23. Borengasser SJ, Zhong Y, Kang P, Lindsey F, Ronis MJ, Badger TM, Gomez-Acevedo H, Shankar K. Maternal obesity enhances white adipose tissue differentiation and alters genome-scale DNA methylation in male rat offspring. Endocrinology. 2013;154(11):4113–25.
24. Li J, Li R, Wang Y, Hu X, Zhao Y, Li L, Feng C, Gu X, Liang F, Lamont SJ, et al. Genome-wide DNA methylome variation in two genetically distinct chicken lines using MethylC-seq. BMC Genomics. 2015;16:851.
25. Zhang S, Shen L, Xia Y, Yang Q, Li X, Tang G, Jiang Y, Wang J, Li M, Zhu L. DNA methylation landscape of fat deposits and fatty acid composition in obese and lean pigs. Sci Rep. 2016;6:35063.
26. Sun Y, Li R, Zhai G, Zhang X, Wang Y. DNA methylation of the PLIN1 promoter downregulates expression in chicken lines. Arch Anim Breed. 2019;62(2):375–82.
27. Zhang Z, Nie C, Chen Y, Dong Y, Lin T. DNA methylation of CpG sites in the chicken KLF7 promoter and exon 2 in association with mRNA expression in abdominal adipose tissue and blood metabolic indicators. BMC Genet. 2020;21(1):120.
28. Cui TT, Huang JX, Ning BL, Mu F, Chen HY, Xing TY, Li H, Wang N. DNA methylation promotes the expression of PPARgamma transcript 1 at least in part by preventing NRF1 binding to the promoter P1 of chicken PPARgamma gene. Poult Sci. 2024;103(5):103559.
29. Huang HY, Liu RR, Zhao GP, Li QH, Zheng MQ, Zhang JJ, Li SF, Liang Z, Wen J. Integrated analysis of MicroRNA and mRNA expression profiles in abdominal adipose tissues in chickens. Sci Rep. 2015;5:16132.
30. Zhang M, Li D, Zhai Y, Wang Z, Ma X, Zhang D, Li G, Han R, Jiang R, Li Z, et al. The landscape of DNA methylation associated with the transcriptomic network of intramuscular adipocytes generates insight into intramuscular fat deposition in chicken. Front Cell Dev Biol. 2020;8:206.
31. Ng AP, Coughlan HD, Hediyeh-Zadeh S, Behrens K, Johanson TM, Low MSY, Bell CC, Gilan O, Chan YC, Kueh AJ, et al. An Erg-driven transcriptional program controls B cell lymphopoiesis. Nat Commun. 2020;11(1):3013.
32. Griffin MJ, Zhou Y, Kang S, Zhang X, Mikkelsen TS, Rosen ED. Early B-cell factor-1 (EBF1) is a key regulator of metabolic and inflammatory signaling pathways in mature adipocytes. J Biol Chem. 2013;288(50):35925–39.
33. Angueira AR, Shapira SN, Ishibashi J, Sampat S, Sostre-Colon J, Emmett MJ, Titchenell PM, Lazar MA, Lim HW, Seale P. Early B cell factor activity controls developmental and adaptive thermogenic gene programming in adipocytes. Cell Rep. 2020;30(9):2869–e28782864.
34. Chao X, Guo L, Wang Q, Huang W, Liu M, Luan K, Jiang J, Lin S, Nie Q, Luo W, et al. miR-429-3p/LPIN1 axis promotes chicken abdominal fat deposition via PPARgamma pathway. Front Cell Dev Biol. 2020;8:595637.
35. Gong P, Jing Y, Liu Y, Wang L, Wu C, Du Z, Li H. Whole-genome bisulfite sequencing of abdominal adipose reveals DNA methylation pattern variations in broiler lines divergently selected for fatness. J Anim Sci. 2021;99(1).
36. Han Y, Han D, Yan Z, Boyd-Kirkup JD, Green CD, Khaitovich P, Han JD. Stress-associated H3K4 methylation accumulates during postnatal development and aging of rhesus macaque brain. Aging Cell. 2012;11(6):1055–64.
37. Kim DY, Lim B, Lim D, Park W, Lee KT, Cho ES, Lim KS, Cheon SN, Choi BH, Park JE et al. Integrative methylome and transcriptome analysis of Porcine abdominal fat indicates changes in fat metabolism and immune responses during different development. J Anim Sci. 2022;100(12).
38. Luo R, Dai X, Zhang L, Li G, Zheng Z. Genome-Wide DNA methylation patterns of muscle and Tail-Fat in dairymeade sheep and Mongolian sheep. Anim (Basel). 2022;12(11).
39. Lu Y, Zhou J, Li F, Cao H, Zhang X, Yu D, He Z, Ji H, Lv K, Wu G et al. The integration of Genome-Wide DNA methylation and transcriptomics identifies the potential genes that regulate the development of skeletal muscles in ducks. Int J Mol Sci. 2023;24(20).
40. Wang S, Zha L, Cui X, Yeh YT, Liu R, Jing J, Shi H, Chen W, Hanover J, Yin J, et al. Epigenetic regulation of hepatic lipid metabolism by DNA methylation. Adv Sci (Weinh). 2023;10(20):e2206068.
41. Gao H, Mejhert N, Fretz JA, Arner E, Lorente-Cebrian S, Ehrlund A, Dahlman-Wright K, Gong X, Stromblad S, Douagi I, et al. Early B cell factor 1 regulates adipocyte morphology and lipolysis in white adipose tissue. Cell Metab. 2014;19(6):981–92.
42. Dang TN, Taylor JL, Kilroy G, Yu Y, Burk DH, Floyd ZE. SIAH2 is expressed in adipocyte precursor cells and interacts with EBF1 and ZFP521 to promote adipogenesis. Obesity. 2020;29(1):98–107.
43. Petrus P, Mejhert N, Gao H, Backdahl J, Arner E, Arner P, Ryden M. Low early B-cell factor 1 (EBF1) activity in human subcutaneous adipose tissue is linked to a pernicious metabolic profile. Diabetes Metab. 2015;41(6):509–12.
44. Brochet P, Ianni BM, Laugier L, Frade AF, Silva Nunes JP, Teixeira PC, Mady C, Ferreira LRP, Ferre Q, Santos RHB, et al. Epigenetic regulation of transcription factor binding motifs promotes Th1 response in Chagas disease cardiomyopathy. Front Immunol. 2022;13:958200.
45. Chu AY, Tin A, Schlosser P, Ko YA, Qiu C, Yao C, Joehanes R, Grams ME, Liang L, Gluck CA, et al. Epigenome-wide association studies identify DNA methylation associated with kidney function. Nat Commun. 2017;8(1):1286.
46. Armartmuntree N, Jusakul A, Sakonsinsiri C, Loilome W, Pinlaor S, Ungarreevittaya P, Yong CH, Techasen A, Imtawil K, Kraiklang R, et al. Promoter hypermethylation of early B cell factor 1 (EBF1) is associated with cholangiocarcinoma progression. J Cancer. 2021;12(9):2673–86.
47. Akerblad P, Mansson R, Lagergren A, Westerlund S, Basta B, Lind U, Thelin A, Gisler R, Liberg D, Nelander S, et al. Gene expression analysis suggests that EBF-1 and PPARgamma2 induce adipogenesis of NIH-3T3 cells with similar efficiency and kinetics. Physiol Genomics. 2005;23(2):206–16.
48. Belarbi Y, Mejhert N, Gao H, Arner P, Ryden M, Kulyte A. MicroRNAs-361-5p and miR-574-5p associate with human adipose morphology and regulate EBF1 expression in white adipose tissue. Mol Cell Endocrinol. 2018;472:50–6.
49. Taniguchi M, Nakajima I, Chikuni K, Kojima M, Awata T, Mikawa S. MicroRNA-33b downregulates the differentiation and development of Porcine preadipocytes. Mol Biol Rep. 2014;41(2):1081–90.
50. Krueger F, Andrews SR. Bismark: a flexible aligner and methylation caller for Bisulfite-Seq applications. Bioinformatics. 2011;27(11):1571–2.
51. Akalin A, Kormaksson M, Li S, Garrett-Bakelman FE, Figueroa ME, Melnick A, Mason CE. MethylKit: a comprehensive R package for the analysis of genome-wide DNA methylation profiles. Genome Biol. 2012;13(10):R87.
52. Li S, Garrett-Bakelman FE, Akalin A, Zumbo P, Levine R, To BL, Lewis ID, Brown AL, D'Andrea RJ, Melnick A, et al. An optimized algorithm for detecting and annotating regional differential methylation. BMC Bioinformatics. 2013;14(Suppl 5):S10.

Publisher's note